ACS APPLIED MATERIALS & INTERFACES

Research Article

www.acsami.org

Highly Sensitive Assay for Acetylcholinesterase Activity and Inhibition Based on a Specifically Reactive Photonic Nanostructure

Tian Tian,‡ Xuesong Li,‡ Jiecheng Cui, Jian Li, Yue Lan, Chen Wang, Meng Zhang, Hui Wang, and Guangtao Li*

Key Lab of Organic Optoelectronics and Molecular Engineering, Department of Chemistry, Tsinghua University, Beijing 100084, China

Supporting Information

ABSTRACT: Assays for acetylcholinesterase (AChE) with high sensitivity and high selectivity as well as facile manipulation have been urgently required in various fields. In this work, a reaction-based photonic strategy was developed for the efficient assay of AChE activity and inhibition based on the synergetic combination of the specific thiol-maleimide addition reaction with photonic porous structure. It was found that various applications including detection of AChE activity, measurement of the related enzymatic kinetics, and screening of inhibitors could be efficiently implemented using such strategy. Remarkably, the unique photonic nanostructure endows the constructed sensing platform with high sensitivity with a limit of detection (LOD) of 5 mU/mL for AChE activity, high selectivity, and self-reporting signaling. Moreover, the label-free solid film-based sensing approach described here has advantages of facile manipulation and bare-eye readout, compared with conventional liquid-phase methods, exhibiting promising potential in practical application for the AChE assay.

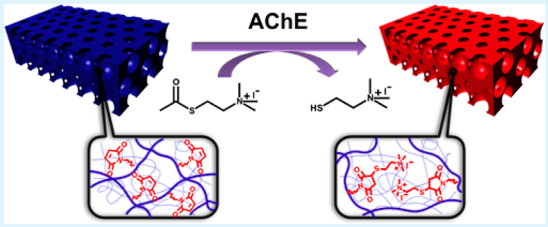

KEYWORDS: *photonic nanostructure, responsive polymer films, reaction-based biosensor, enzyme assay, acetylcholinesterase*

1. INTRODUCTION

As a ubiquitous enzyme in the nervous system, acetylcholinesterase (AChE) plays a crucial role in biological signal transmission,[1] which mainly functions to terminate the synaptic transmission of neurotransmitter acetylcholine (ACh) by means of hydrolyzing ACh to choline and acetate.[2,3] Inhibition of AChE activity would cause accumulation of ACh in a synaptic cleft, resulting in hindered neurotransmission.[4,5] Regulating the activity of AChE would have great impact on physiological function. Reversible inhibitors of AChE are widely used in therapies for Alzheimer's disease (AD),[6] while irreversible inhibitors, such as nerve gas, would cause asphyxiation or even death.[7,8] Therefore, the development of efficient approaches for AChE activity measurement with high sensitivity, fast response, and facile manipulation is of high importance on both theoretical and practical aspects and has been urgently needed for fields including clinic diagnosis and AD drug screening as well as organophosphorus pesticide detection.[9]

The most widely used assays for AChE activity include the colorimetric assay using Ellman's reagent and chemolumiscence detection by cascade hydrolysis-oxidation of ACh.[10,11] Such methods would suffer from relative low sensitivity, long time consumption, and false positive results.[12] Recently, a number of approaches has been implemented to obtain better performance of AChE activity measurement, including single-molecule fluorescent probes,[13] gold nanoparticle (Au-NP) plasmonics,[14,15] aggregation-induced emission (AIE),[16] colorimetric and fluorescent change of conjugate polymers,[17,18] and modified electrochemical methods.[19,20] Notable performances have also been achieved in several cases. Nevertheless, non-neglectable obstacles or drawbacks still exist during practical application. The electrostatic interaction involved in a vast majority of these methods would be influenced by aqueous electrolytes. Self-quenching and bleaching phenomena have long been known for fluorescent probes or conjugate polymers, potentially causing false results. Although Au-NP owns relatively high sensitivity, its performance might be limited by competitive binding of biomolecules and fast nondirective aggregation in a complex sample.[21−23] Moreover, most of the existing approaches are implemented in liquid phase, lacking the feature of convenient manipulation, which is more favorable for practical application.[24] Therefore, developing a novel strategy for the high-performance AChE assay overcoming these limitations is of significant current interest.

In this work, a reaction-based photonic strategy is developed for efficient assay of AChE activity and inhibition based on the synergetic combination of the specific thiol-maleimide addition reaction with photonic porous structure. Various applications including detection of AChE activity, measurement of the related enzymatic kinetics, and screening of inhibitors could be efficiently implemented using such strategy. Remarkably, the unique photonic nanostructure endows the constructed sensing platform with high sensitivity with a limit of detection (LOD)

Received: June 24, 2014
Accepted: August 18, 2014
Published: August 18, 2014

of 5 mU/mL for AChE activity, high selectivity, and self-reporting signaling. Furthermore, the label-free solid film-based sensing approach described here has advantages of facile manipulation and bare-eye readout, compared with conventional liquid-phase methods, exhibiting promising potential in practical application for the AChE assay. A schematic diagram for the fabrication and mechanism of the photonic sensing platform is proposed in Scheme 1.

Scheme 1. Schematic Illustration of the Fabrication and Mechanism of the Reaction-Based Photonic Platform for Sensing AChE Activity and Inhibition

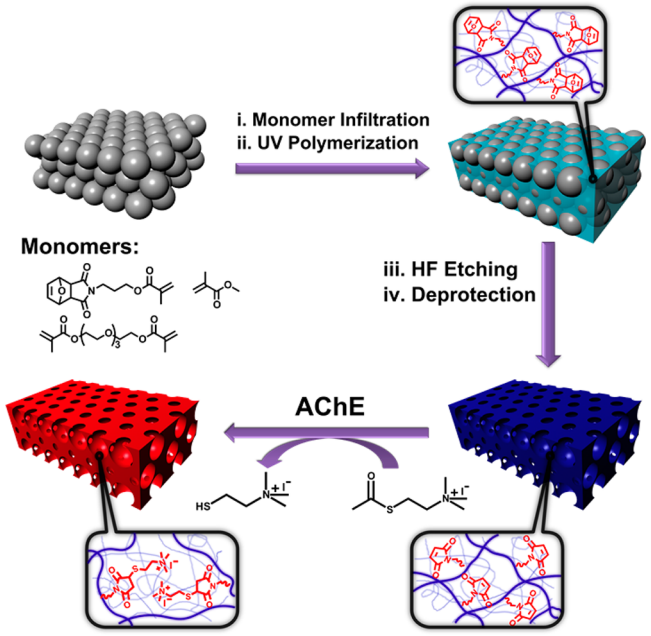

2. EXPERIMENTAL SECTION

Chemicals. All of the chemicals and solvents used in the experiments were of reagent quality, without further purification unless mentioned. Anhydrous ethanol, ammonia, acrylic acid, tetraethoxysilane (TEOS), and dichloromethane were all purchase from SinoChem co. Ltd. Methyl methacrylate, tetraethylene glycol dimethacrylate (TEGDMA), and photoinitiator 2-hydroxy-2-methyl-1-phenyl-1-propanone (HMPP) were purchased from Acros Organics. Exo-3,6-epoxy-1,2,3,6-tetrahydrophthalic anhydride and 3-amino-1-propanol were obtained from Alfa Aesar. Acetylthiocholine iodide, acetylcholinesterase, butylcholinesterase, lysozyme, propidium iodide, tacrine, and donepezil were bought from Sigma-Aldrich. PBS buffer solution, methacryloyl chloride, and other affiliated chemicals were supplied by local suppliers. The flasks for Stöber silica sphere synthesis were treated by dichromate lotion before use. All glass slides were sheared out to be 50 mm × 20 mm, following piranha treatment, and rinsed with deionized water and anhydrous ethanol.

Characterization Methods. The ^{1}H NMR spectra of substances were characterized by a JEOL ECA 300 NMR spectrometer. Reflectance spectra of photonic samples were measured by a USB200 fiber spectrometer (Ocean Optics). The SEM images were taken by a LEO-1503 field emission scanning electron microscope.

Synthesis of Functional Monomer. The synthesis of the maleimide-functional monomer followed the route as shown in Scheme 2.

Synthesis of Compound 1. Exo-3,6-epoxy-1,2,3,6-tetrahydrophthalic anhydride (3.32 g, 20 mmol, 1 eqiv) and 3-amino-1-propanol (7.50 g, 100 mmol, 5 eqiv) were heated without solvent at 80 °C coupled by vigorous stirring for 4 h. The mixture was dissolved in CH_2Cl_2 and then washed with dilute HCl and saturated brine, respectively. The organic layer was dried by anhydrous $MgSO_4$ and concentrated by vacuum evaporation. A white solid was obtained (1.59 g, 35.7%). Compound **1**: 2-(3-hydroxypropyl)-3a,4,7,7a-tetrahydro-1*H*-4,7-epoxyisoindole-1,3(2*H*)-dione. ^{1}H NMR (300 MHz, $CDCl_3$): δ 6.53 (s, 2H, −CH═), 5.28 (s, 2H, −CH−O−), 3.65 (t, −N−CH_2−, 2H), 3.53 (t, −CH_2−O−, 2H), 2.88 (m, 2H, −CHCO−), 2.50 (s, 1H, −OH), 1.77 (m, 2H, −$CH_2CH_2CH_2$−).

Synthesis of Compound 2. Compound **1** (0.90 g, 4.04 mmol, 1 eqiv) was dissolved in CH_2Cl_2 and placed in an ice bath. A solution of methacryloyl chloride (0.50 g, 4.84 mmol, 1.2 eqiv) in CH_2Cl_2 was added dropwise within 5 min. The mixture was kept at room temperature overnight for complete reaction. The mixture was washed with water and saturated brine twice, dried, and purified by a flash chromatographic column (2:1 v/v hexane/ethyl ester). The product obtained was a white waxy solid (1.03 g, 87.5%). Compound **2**: 3-(1,3-dioxo-3a,4,7,7a-tetrahydro-1*H*-4,7-epoxyisoindol-2(3*H*)-yl)-propyl methacrylate. ^{1}H NMR (300 MHz, $CDCl_3$): δ 6.51 (s, 2H, −CH═CH−), 6.13 (s, 1H, ═CH_2), 5.57 (s, 1H, ═CH_2), 5.26 (s, 2H, −CHO−), 4.12 (t, 3H, −CONCH_2−), 3.61 (t, 3H,

Scheme 2. Synthesis Scheme of Furan-Protected Maleimide Functional Monomer

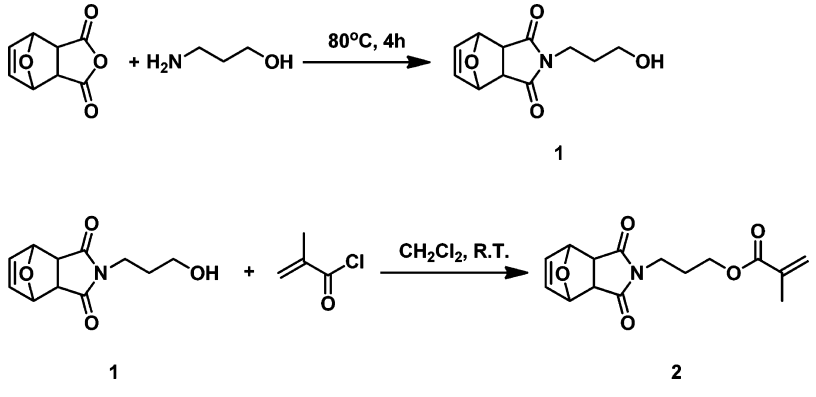

dx.doi.org/10.1021/am504065v | ACS Appl. Mater. Interfaces 2014, 6, 15456−15465

$-COOCH_2-$), 2.84 (m, 2H, $-CHCO-$), 1.97 (m, 5H, $-CH_3-CH_2-$).

Preparation of SiO_2 Colloid Crystal Templates. The monodisperse silica particles were synthesized following the Stöber method. Ammonia (10−14 mL) and 120 mL of anhydrous ethanol were poured into a flask equipped with a magnetic beater. After being mixed uniformly, 4 mL of TEOS was slowly added dropwise. The mixture was stirred at room temperature for ca. 5 h. Monodisperse SiO_2 spheres with diameter ranging from 200 to 300 nm were obtained after centrifugation and dispersion in anhydrous ethanol for several times to remove the residues. In most cases, silica particles of 270−290 nm were used. Afterward, the obtained SiO_2 spheres, dispersed in anhydrous ethanol with a weight concentration of about 1−4%, were allotted into 10 mL cleaning vials. A glass slide treated with H_2SO_4/H_2O_2 was inserted vertically. The vials were kept in an oven of constant temperature for weeks. After the complete evaporation of the solvent, the colloidal dispersion slowly traced down the surface of the glass slides, coated by SiO_2 spheres, which could assemble into a face-cubic-center (fcc) crystal arrangement driven by capillary force.

Preparation of Inverse Opal Polymer Films Containing Maleimide Pendants. The inverse opal photonic films containing maleimide pendants were prepared via template infiltration, polymerization, and an etching process. An assortment of precursors prepared by mixing predetermined proportions of functional monomer (0.289 g, 1 mmol), MMA (0.100 g, 1 mmol), TEGDMA (0.152 g, 0.5 mmol), and photoinitiator HMPP (1% molecular fraction) were infiltrated into a clamped mixture of glass slide and silica template, until the template became totally transparent. The precursors were then polymerized by UV exposure (500 W lamp at 30 cm distance) for 10 min. After etching SiO_2 with 1% HF, the inverse opal film containing maleimide pendants protected with furan was obtained. The protected film was refluxed in toluene under 110 °C for 5 h and taken out immediately after heating was stopped, in order to prevent the reversible Diels−Alder addition. The polymer film was then washed with a mixture of alcohol and water and was immersed into deionized water before use. In the case of SEM characterization of the hexagonal structure, a sample of inverse opal is treated with ionic plasma to remove polymer overlayer on the surface.

Characterizations of the Photonic Films in Response to Acetylcholinesterase. In general, the obtained photonic films were cut into 3 × 3 mm^2 and transferred onto a black adhesive tape. The tape was further settled on the bottom of a 1 mL polypropylene tube (for sequential analysis, a 96-well plate was favored). A solution of AChE, ATCh, or AChE inhibitors was balanced to 1 mL and injected into the tube. Reflectance spectra were taken from the top side of the tube. Detailed conditions for different applications were given as follows: (i) For measurement of photonic response to varied concentration of enzyme, the concentration of ATCh was constant at 1 mM, and concentrations of AChE were varied from 10 mU/mL to 10 U/mL. Reflectance spectra were measured over 30 min after incubation for high concentrations, while at low concentrations (10^{-7}−10^{-9} M), the Bragg diffraction peak was monitored until no further change was observed. (ii) For the selectivity assay, the concentration of ATCh was 1 mM, while AChE, BChE, and lysozyme are employed as 10 U/mL, respectively. Reflectance spectra were measured over 30 min after incubation as well; considering the enzyme activity in the experiment, nearly all the substrates would be hydrolyzed in a time span of 30 min. (iii) For enzymatic kinetics measurement, 1 U/mL AChE was used. Time series of spectra under four substrate concentrations (5 × 10^{-6}, 1 × 10^{-6}, 5 × 10^{-7}, and 2 × 10^{-7} mol/L) were recorded, and initial velocities were calculated by the slope of the linear fitting curve of the first three data points.

Screening of Inhibitors via the Fabricated Photonic Films. The solutions of AChE and the inhibitors (propidium iodide, tacrine and donepezil) of varying concentration (10^{-9}−10^{-4} mol/L) were incubated at room temperature for 30 min for binding; then, the substrate acetylthiocholine and the fabricated photonic film were added, and the mixtures were left for over 30 min to allow hydrolysis and click reaction to take place.

3. RESULTS AND DISCUSSION

Herein, we present a reaction-based photonic strategy for AChE activity measurement, utilizing maleimide-containing reactive three-dimensional (3D) inverse opal polymer films as the sensing platform. 3D inverse opal films are photonic materials with 3D periodicity in nanoscale structure and refractive index.[25,26] Due to the unique photonic band gap (PBG) structure of 3D photonic crystal, only the light within a narrow range of wavelength can be reflected. As demonstrated in eq 1, under normal incidence geometry, the wavelength λ of maximum reflection is a function of lattice spacing (d) and effective refractive index (n_{eff}):[27]

$$\lambda = 1.633 n_{eff} d \quad (1)$$

Polymer-based stimuli-responsive photonic crystals have been employed for chemical and biological sensing in recent years[28,29] due to the sensitivity brought by both photonic periodic structure and responsiveness of polymer material. The main principle behind such photonic sensing lies in the optical property change brought by external stimuli. As shown in eq 1, either the change of material reflective index or the lattice spacing would result in the shift of the Bragg diffraction wavelength. The optical signal generation is self-reporting, videlicet, requiring no fluorescent probing molecules. By employing the volume-transition feature of stimuli-responsive polymer, series of photonic crystal sensing assays have been proposed, responding to various types of external stimuli.[30−35] In this respect, a few examples of photonic methods concerning AChE have been reported.[36,37] The Asher group developed a polymerized crystalline colloidal array (PCCA) with attached AChE and used it as sensing material for detection of the organophosphorus compound parathion.[36] On the other hand, the Lowe group described a double-layer structured holographic sensor as a label-free detection system, and by using AChE as the model enzyme, holographic inhibition assays for drug discovery were demonstrated.[37] However, both cases yet require cumbersome immobilization of AChE.

It would be more facile to operate with AChE in the bulk, in which case the enzyme activity of AChE would not be affected by chemical modification. In our case, the activity sensing of AChE was carried out in the form of measuring the hydrolysis of substrate acetylthiocholine (ATCh). The thiol-containing product thiocholine (TCh) was the *defacto* molecule detected in this system (see Scheme 1). Benefitting from the well-established thiol-maleimide Michael addition reaction,[38−40] the polymer photonic crystal should be selectively responsive to thiol compounds by introducing maleimide pedants. As illustrated in Scheme 1, a responsive polymer inverse opal was obtained by copolymerization of a furan-protected

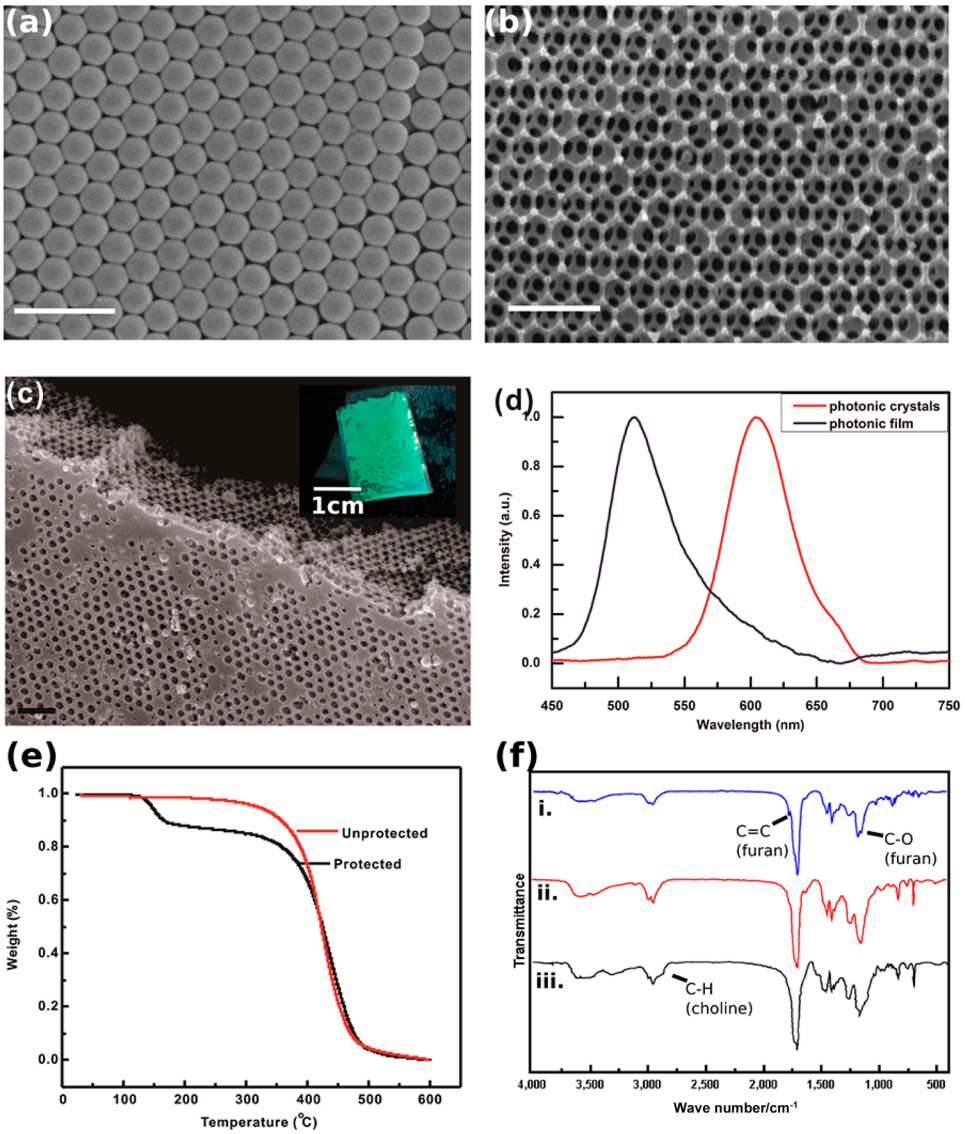

Figure 1. SEM images of colloidal crystal template (a), the resultant maleimide-containing inverse opal film (b), and its cross-section view (c); inset illustrates the optical picture of an uncut fabricated film. All scale bars except the one in the inset are 1 μm. (d) Reflection spectra of the colloidal crystal template and the inverse opal film. (e) TGA curves of the furan-protected and deprotected films. (f) IR spectra of furan-protected film (i), deprotected film (ii), and the film reacted with TCh (iii).

maleimide-containing monomer (Scheme 2) with methyl methacrylate (MMA) and tetraethylene glycol dimethacrylate (TEGDMA) as cross-linker in the voids of 3D silica colloidal crystal template, followed by etching of the silica template using diluted hydrofluoric acid, and deprotection of maleimide pedants by heating. The resultant inverse opal polymer film was reactive to thiol compounds. While in absence of AChE, ATCh was stable against the polymer; however, upon its hydrolysis, the product TCh would rapidly react with the maleimide moieties within. Distinguished from the original hydrophobic polymer, the TCh-attached polymer possessed increased charge due to the positive-charged quaternary ammonium group. An elevated Donan potential was thus produced, driving water into the polymer and finally leading to the volume transition of the photonic polymer film. The expansion of polymer lattice spacing due to swelling would red-shift the PBG wavelength, generating a signal which could be detected using a reflection spectrometer or even the bare eye. Thus, the reaction-based recognition event can be directly transferred (label-free) into a readable optical signal through a change in Bragg diffraction of the ordered photonic film (self-reporting signaling). It should be noted that the peak shift is affected by the concentration of attached TCh, revealed by the Flory's theory of gel swelling.[41] Once the correlation between the optic signal and TCh concentration has been established, it is feasible to detect the enzymatic activity of AChE using such a platform as pH paper.

In principle, two major factors are responsible for the peak shift signal: chemical condensation between maleimide and thiol groups; osmotic pressure change before and after the condensation. The specific reaction of maleimide with thiol groups is fast and stoichiometric even for polymer in a mild condition,[40] ensuring the specificity of such photonic sensing platform. The "click-reaction" feature ensures reliable sensing of thiol compounds in aqueous solution, while getting rid of influence of nonspecific electrolytes. Distinguishing TCh from other thiol-compounds can be possible due to the second factor. Bearing a quaternary ammonium group, TCh shows

constant charge independent of solution pH, while most of the other biothiols, e.g., cysteine and glutathione, exhibit attenuated charge under certain pH. The influence of other amino-acid-derived thiols could be ruled out by performing a series of spectra under varied pH values.[42]Besides self-reporting signaling feature and high selectivity, the unique photonic structure also guarantees the high sensitivity of the assay both by the enrichment effect through the stoichiometry of the reaction and the high specific area of porous structure, as revealed by related works using photonic crystal as the sensing platform.[36,43]

Additionally, utilizing a solid-film-based sensor owns a series of advantages including convenient manipulation, long shelf life, and reduced inhibition of enzyme, compared with liquid-state, small-molecular probes. Although molecule transportation is slower inside of the solid material than the aqueous solution system, the interconnected macroporosity of inverse opal gives compensation, ensuring a much faster response than bulk polymer.[44] Unlike other film sensors coupled with electrode, the detection platform proposed in this work is energy-free and the self-reporting optical signaling could be determined even by the bare eye, which is promising for practical application. Detailed experimental results and discussions are presented in the following sections, in order to explore the performance and application feasibility of such a sensing system.

The periodicity of photonic crystal was successfully acquired after the template-assisted fabrication process. As shown in Figure 1, both the SEM photographs of silica colloidal crystal template (Figure 1a) and fabricated inverse opal polymer (Figure 1b) showed close-packed hexagonal arrangement with little deviation in lattice spacing. A tilted angle view image in Figure 1c further proved that the periodicity was uniform in the polymer slab constructed of ca. 20 layers. As shown in Figure 1d, the photonic crystal template constructed of ca. 300 nm silica nanospheres had a diffraction peak wavelength of 605 nm, while for the resultant inverse opal polymer film, the peak wavelength blue-shifted to ca. 512 nm. Despite minor defects and polymer overlayers, the inverse opal polymer still exhibited relatively high optical quality with a half-peak width of 57.7 nm and a Q factor of 8.82.

Since the double bond in maleimide is unstable during the radical polymerization process, it is necessary to protect the maleimide groups before final deployment. A commonly used strategy is to employ the furan-protected maleimide compounds. By heating the polymer in nonpolar solvent such as toluene, a reverse Diels–Alder reaction would take place, yielding unprotected maleimide pedants. Thermogravimetric analysis (TGA) was utilized to verify the complete deprotection. According to the TGA curves in Figure 1e, the protected inverse opal polymer exhibited a loss of ca. 10% weight from 100 to 200 °C, corresponding to the releasing of furan molecules. However, the treated polymer had no observable weight loss until a normal decomposition temperature at 400 °C, proving that the deprotection process was completed. Meanwhile, infrared (IR) spectra in Figure 1f also provided evidence for the deprotection. The C–O stretching vibration of ether groups in the protected polymer of ca. 1158 cm^{-1} was decreased in the treated polymer; the C=C bending vibration of furan at 1783 cm^{-1} in the protected polymer was also absent after deprotection.[45] By combination of the IR and TGA analysis, the deprotection process was proved to be complete.

To explore the reaction feasibility of the photonic sensing platform, a piece of deprotected inverse opal film was dipped into a PBS buffer (pH = 7.4) containing 1 mM ATCh and 10 U/mL AChE for 30 min. IR and contact angle tests were performed to verify the reaction in the film. It should be noted that the weak vibration peak of C=C of maleimide is overlapped by that of C=O, which could not be reliable for verifying the reaction.[46] The emergence of a shoulder peak at 2869 cm^{-1} of the reacted sample should be ascribed to the C–H vibration of the thiocholine adducts. Contact angle measurements were also carried out as macroscale verification for the polymer films before and after ATCh hydrolysis. As shown in Figure S1, Supporting Information, the original hydrophobic polymer film turned quite hydrophilic upon reaction with 10 U/mL AChE, with the contact angle sharply deceased from 85.9° to 8°. Considering all possible species in the system, the drastic change in hydrophilicity could only be the consequence of increased charge of the polymer. The gradual immersion of a water drop on the surface of the film shown in Figure S1c, Supporting Information, further supported the existence of inner macropores, in contrast with a simple planar surface in Figure S1a, Supporting Information.

We further studied the detectability of the photonic sensing platform. As the enzyme reaction is time dependent, a series of time-dependent experiments under varied concentrations was performed in order to determine the reaction time required for a steady state (Figure S4, Supporting Information). Over a time span of 30 min, the Bragg diffraction peak reached equilibrium for high and medium concentrations (10^{-3} and 10^{-6} M), while for a lower concentration (10^{-9} M), the peak shift was also over 90% of its full shift. Thus, the reaction time was chosen to be 30 min for high and medium concentrations, while for lower concentrations, the peak shift was monitored until its maximum. The intensities of all the spectra were normalized for convenience of further comparison. As revealed in Figure 2a, the original inverse opal polymer film exhibited a Bragg diffraction peak at 505.7 nm. The reflection spectra showed a drastic change upon AChE enzymatic reaction. Immersion of the film into a PBS buffer of 2.5 U/mL AChE and 1 mM ATCh led to a red-shift of the peak wavelength to 569.3 nm, while under 10 U/mL AChE, the wavelength further increased to 634.4 nm. Indicated by the insets of optical images in Figure 2a, the color change of the polymer film could be detected by the bare eye. A systematic survey of detection capacity was carried out using AChE of diverse concentrations ranging from 10 mU/mL to 10 U/mL, while the concentration of ATCh was fixed to be 1 mM. It could be observed that the Bragg diffraction peak shift attenuated following the decrease of AChE concentration (Figure 2b). The peak shift was plotted against the AChE concentration (Figure 2c), and the limit of detection (LOD) of AChE was calculated as 5 mU/mL, extending the curve at low concentration to a minimal detectable peak shift of 6 nm (3 times the signal fluctuation of the optical spectrometer). The achieved LOD challenged those of established methods,[47] including Au-NP plasmonics[14] and AIE fluorescence,[16] and even overwhelmed most of the methods based on conjugate polymer colorimetric assays or fluorescence.[17,18] The high sensitivity could be attributed to both the properties of inverse opal photonic structure and the reactive polymer. Since the structural color of photonic crystals is only governed by the polymer structure and lattice quality, there would be no undesired influence like the self-quenching or bleaching of the fluorescence-based sensory systems,

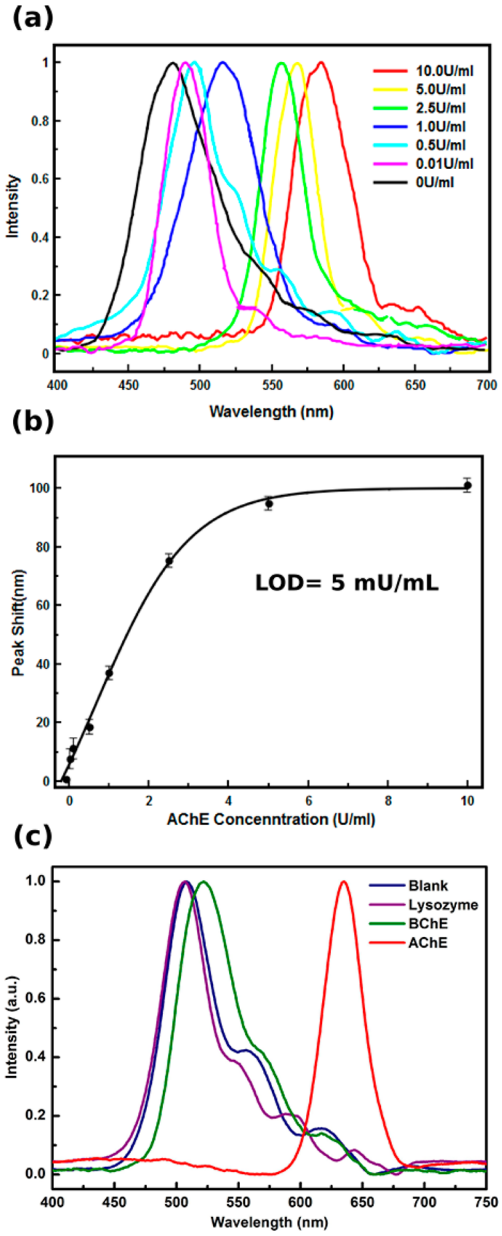

Figure 2. (a) Reflection spectra of the photonic film under varied AChE concentrations. (b) The dependency of the Bragg peak shift with AChE concentration. A LOD of 5 mU/mL was calculated. (c) Reflection spectra of the photonic film with lysozyme, BChE, and AChE.

ensuring a relative low background noise. Moreover, the polymer underwent a steep hydrophilicity change upon the TCh addition reaction, which yielded a photonic signal even with a low level of TCh (see Appendix in Supporting Information). Since the TCh molecules were immobilized after the addition, the charge within the polymer would also remain constant against rinsing. Such an encouraging result implied a strong potential in the detection of AChE activity and related application areas for the photonic sensing platform.

With the proposed sensing strategy feasible, we further examined its specificity against other enzymes. Lysozyme (Lyz), butylcholinesterase (BChE), and AChE were employed for comparison of sensing specificity. Photonic polymers of identical size were immersed into PBS buffer solutions containing ATCh and different enzymes, respectively. The concentration of ATCh was maintained constant at 1 mM, and all enzyme concentrations were as great as 10 U/mL. As demonstrated in Figure 2d, merely no peak shift from the control experiments could be observed for Lyz. In the case of BChE, there was also only minor peak shift, compared with the significant change by using AChE. The high selectivity of the fabricated photonic sensing platform evidently contributed to the high selectivity of the substrate ATCh with its corresponding enzyme AChE. AChE, BChE, and Lyz are all capable of hydrolysis of ester substances. However, in the case of ATCh as the substrate, the discrimination of enzyme specificity is clearly shown. Alternatively, the specificity of AChE with other thioesters reduces the influence of false positive results.[48] Therefore, the combination of the maleimide containing photonic film together with acetylthiocholine constructed an ideal sensing platform, which would only be due to the existence of AChE.

It is hopeful that various applications could be developed from the fabricated photonic sensing platform, due to its benefits of high sensitivity and specificity. Using the time-resolved assay, one could study the enzyme kinetics of AChE. The key point was the translation of the peak shift signal into the concentration of the hydrolysis product TCh. In order to retrieve the correlation between the concentration of TCh and the Braggs peak shift, a series of measurements was performed under varied concentration of TCh ranging from 1 nM to 1 mM (Figure 3a). The Bragg diffraction peak was observed to expand after increasing ATCh concentration. During the reaction process, there could be an intermediate phase in which the polymer is partially ionized. According to eq 1, the lattice spacing d is not uniform in such a stage, which would contribute to the broadening of the Bragg diffraction peak. As concentration increases, the Bragg diffraction peak sharpened as ionization ratio increased. In the case of high hydrophilic polymer, the ununiform swelling caused by defects would further amplify the defects, resulting in a broadening of the Bragg diffraction peak. In fitting of the working curve, both quadratic and sigmoidal functions were used. Although the sigmoidal fitting had better theoretical enzyme models, it was found that the quadratic fitting had a better performance with higher R^2 values (Figure S5, Supporting Information). Therefore, a quadratic curve was fitted to generate the working curve of logged hydrolyzed ATCh concentration versus Bragg diffraction peak shift (Figure 3b). Although a quantitative model for such a plot failed, a qualitative interpretation could be given. At low concentration of TCh, the increase of polymer ionization ratio would yield a great change of polymer hydrophilicity, turning the polymer from hydrophobic to hydrophilic; while the concentration of TCh further increased, the addition in hydrophilicity caused by the concentration of TCh became less. For the quadratic plot, the slop of tangent (e.g., the derivative of the quadratic function) decreased as log C increased, consistent with the real situation. In order to examine the kinetics of AChE, a Lineweaver–Burk curve with double reciprocals of initial velocity $(1/V_0)$ versus substrate concentration $(1/[S_0])$ was plotted.[49] The initial velocity was calculated as the slope of the initial region (which was chosen as the five data points of the first 300 s) of the time curve of ATCh hydrolysis, which was converted from the time-resolved spectra (Figure S2, Supporting Information). The Lineweaver–Burk plot can be employed to reveal the enzyme kinetics of AChE. When one calculates the slope and the intercept, the Michaelis–Menten constant (K_m) and maximum velocity (V_m)

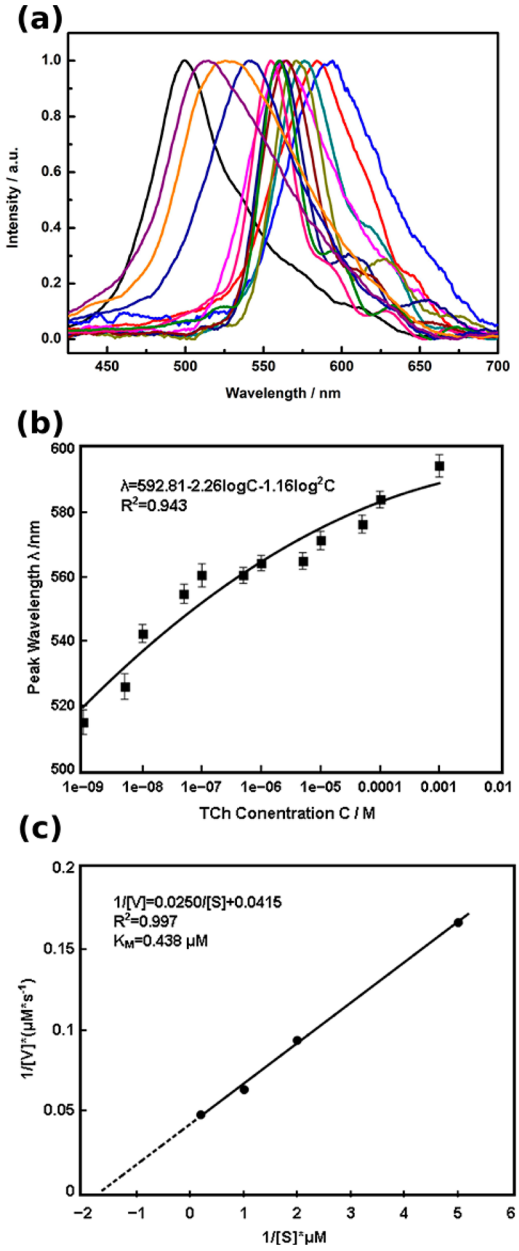

Figure 3. (a) Reflection spectra of the photonic film against varied concentration of TCh. (b) Standard working curve derived from (a). (c) Lineweaver–Burk plot of AChE kinetics.

can be obtained. In our case, the V_m was calculated as 40.0 μM/s and K_m as 0.438 μM from the Lineweaver–Burk plot as shown in Figure 3c. Notably, the apparent K_M value was significantly lower than that of using small-molecular probe approaches.[17,50] A plausible explanation for the apparent acceleration of enzyme kinetics was the prevention of enzyme inhibition, since the detection for AChE activity involving small-molecular probes or even synthesized ACh analogues would induce inhibition of the enzyme. However, as a polymer material enriching the hydrolysis product of the substrate, the fabricated photonic polymer possesses little interference with the enzyme active sites, significantly reducing the inhibition effect. Also, the calculated initial velocity used the data spots from 60 to 300 s, which could be slightly higher than real initial velocity. Moreover, the interconnected porous structure of the inverse opal photonic film ensures fast matter diffusion within, abating the bias caused by the slow response rate related to solid detectors. Due to the macroporous structure of the photonic crystal, the mass transfer of hydrolysis product TCh is accelerated compared with bulk polymer. At relatively low concentrations, it was inferred that the reaction mainly took place at the surface of the macroporous polymer. Meanwhile, since the monitored time here was 5 min for the initial velocity measurement, the further diffusion of substance into the polymer interior was minor compared with the reaction at the polymer surface. Together with the fast reaction property of the thio-maleimide reaction, the response of lower concentration could be avoided.

Similar to the measurement of enzyme activity under normal conditions, it is possible to determine the inhibition of the enzyme, providing a facile and clear method of AChE inhibitor screening. Three kinds of commonly used inhibitors, propidium iodide, tacrine, and donepezil, were selected for demonstration. In the inhibition assays, solutions of AChE (10 U/mL) and the inhibitors of diverse concentrations (10^{-4}–10^{-9} M) were incubated at room temperature for 30 min to reach the binding equilibrium. The mixture was added to the kit containing substrate ATCh (1 mM) and the inverse opal film in PBS buffer for 30 min before detection of the final peak-shift. The inhibition ability was described by the IC_{50} value, referring to the inhibitor concentration required for 50% inhibition of enzyme activity. The IC_{50} value was obtained from the plot of inhibition efficiency (IE) versus inhibitor concentration. Expressed by eq 2, the IE value is the ratio of substrate concentration change under the inhibited condition to that under the normal condition and is equivalent to the ratio of hydrolyzed substrate concentration under inhibited and normal conditions. It is acceptable to assume the hydrolyzed ATCh concentration under such level of AChE was equal to that of the initial concentration under a time span of 30 min.

$$\mathrm{IE} = \frac{c_0 - c_i}{c_0 - c_n} = \frac{c_{\mathrm{hydro,i}}}{c_{\mathrm{hydro,n}}} \approx \frac{c_{\mathrm{hydro,i}}}{c_0} \qquad (2)$$

Spectra of the photonic sensing film with inhibitor of varied concentration were measured, as illustrated in Figure S3, Supporting Information. For each inhibitor, the IE (i.e., the ratio of current peak shift with full peak shift without the inhibitor) of the photonic film was plotted against its concentration in order to retrieve the IC_{50} value. The three kinds of inhibitors, propidium iodide, tacrine, and donepezil, exhibited inhibition capacities of AChE with IC_{50} values of 43.4, 9.98, and 2.43 nM, respectively (Figure 4a–c). The screening application using the fabricated photonic sensing platform possesses universality for either reversible inhibitors, like drugs for Alzheimer's disease, or even hazardous irreversible inhibitors, providing a promising potential for a wide range of fields, including pharmaceutical research, clinical diagnostics, etc.

Thanks to the combination of optical features of photonic crystal with a specific reaction, the photonic sensing platform appeared to be promising for AChE activity measurement and related inhibitor screening with notable sensitivity and specificity. Additional features drive it toward applications for a wide-range of samples. Additionally, the stability of the photonic film against rinsing would reduce the influence of naturally existing solutes, compared with conventional liquid-phase assay methods.[36] As mentioned above, deprived of the nondirectional electrostatic interaction, the platform described

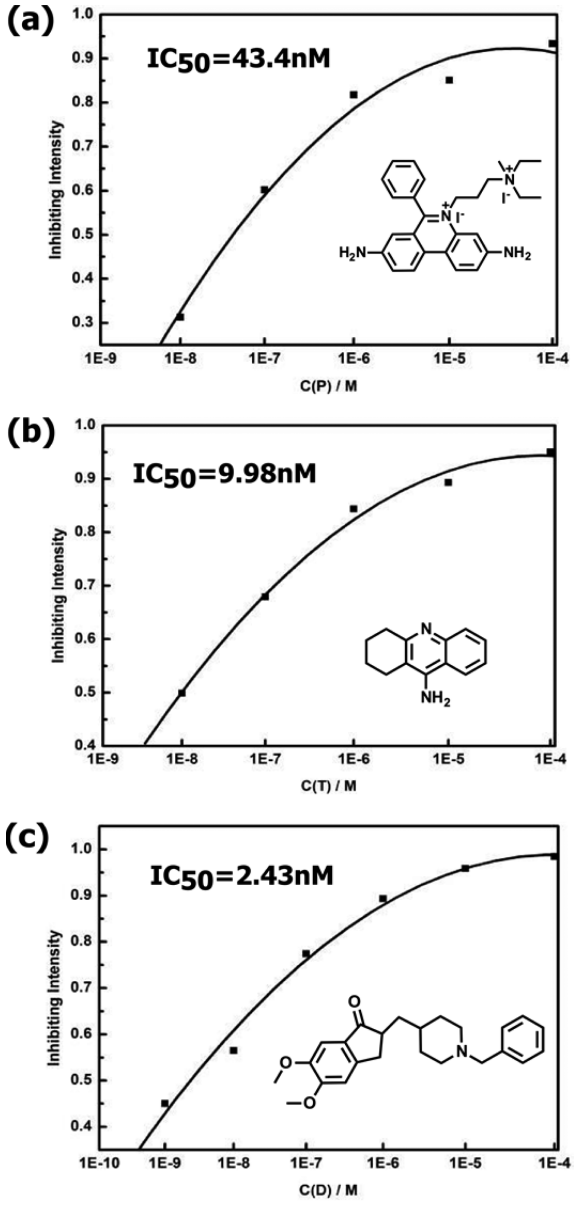

Figure 4. Inhibition curve of propidium iodide (a), tacrine (b), and donepezil (c), respectively.

here specifically responds to thiol-containing and charged species, largely reducing the possibility of false positive results. Although the LOD appeared to be slightly poorer than the most sensitive approaches such as amplified Au-NP plasmonics and a single molecular fluorescence probe, the sensing platform performed far beyond the need for practical application[9] and still ranks among the top of the related methods. Although the concept of using a photonic crystal for biomolecule sensing has emerged for several years,[51−53] our system is capable for more complex applications concerning enzyme activity and inhibitor sensing. The inverse opal type photonic crystal ensures better mechanical strength than the embedded colloidal array. Employing reaction-based responsive polymer would also be more dependable than nondirectional molecular imprinting, taking the specificity into account.

4. CONCLUSION

In summary, an efficient photonic assay strategy for AChE activity and inhibition has been developed on the basis of the synergetic combination of photonic nanostructure with the specific addition reaction of maleimide with enzymatic hydrolysis product TCh. Arising from the combination of the specific reaction and unique properties of photonic macroporous film, the constructed sensors enable a highly sensitive and selective detection of AChE under ambient conditions with a self-reporting feature and no need to use any labels. Moreover, the developed sensor could efficiently perform the measurement of the related enzyme kinetics and inhibitor screening. Benefiting from the reliability against electrolyte, easy handling, low cost, and bare-eye-readable optical signal, our sensory system shows great potential in practical application for the AChE assay. We believe in the promising outlook that such reaction-based photonic assay strategy could also be extended to other important fields like pharmaceutical research, clinical diagnosis, and environment monitoring.

■ ASSOCIATED CONTENT

Ⓢ Supporting Information

A photograph for the contact-angle test, raw spectra data for kinetics and inhibitor screening, and a brief discussion for the detection capacity of this photonic material. This material is available free of charge via the Internet at http://pubs.acs.org.

■ AUTHOR INFORMATION

Corresponding Author

*E-mail: lgt@mail.tsinghua.edu.cn.

Author Contributions

‡T.T. and X.L. contributed equally.

Notes

The authors declare no competing financial interest.

■ ACKNOWLEDGMENTS

We gratefully acknowledge the financial support from the NSF China (21025311, 21121004, and 91027016), MOST Programs (2011CB808403 and 2013CB834502), and the Deutsche Forschungsgemeinschaft DFG (TRR61).

■ ABBREVIATIONS

AChE, acetylcholinesterase
ACh, acetylcholine
ATCh, acetylthiocholine
TCh, thiocholine
Lyz, lysozyme
BChE, butylcholinesterase
LOD, limit of detection
Au-NP, gold nanoparticle
AIE, aggregation-induced emission
TGA, thermogravimetric analysis

■ REFERENCES

(1) Quinn, D. M. Acetylcholinesterase: Enzyme Structure, Reaction Dynamics, and Virtual Transition States. *Chem. Rev.* **1987**, *87*, 955−979.

(2) Whittaker, V. P. The Contribution of Drugs and Toxins to Understanding of Cholinergic Function. *Trends Pharmacol. Sci.* **1990**, *11*, 8−13.

(3) Ballard, C. G. Advances in the Treatment of Alzheimer's Disease: Benefits of Dual Cholinesterase Inhibition. *Eur. Neurol.* **2002**, *47*, 64−70.
(4) Ashani, Y.; Peggins, J. O., III; Doctor, B. P. Mechanism of Inhibition of Cholinesterases by Huperzine A. *Biochem. Biophys. Res. Commun.* **1992**, *184*, 719−726.
(5) Tougu, V. Acetylcholinesterase: Mechanism of Catalysis and Inhibition. *Curr. Med. Chem.: Cent. Nerv. Syst. Agents* **2001**, *1*, 155−170.
(6) Bartolini, M.; Bertucci, C.; Cavrini, V.; Andrisano, V. β-Amyloid Aggregation Induced by Human Acetylcholinesterase: Inhibition Studies. *Biochem. Pharmacol.* **2003**, *65*, 407−416.
(7) Pope, C. N. Organophosphorus Pesticides: Do They All Have the Same Mechanism of Toxicity? *J. Toxicol. Environ. Health, B* **1999**, *2*, 161−181.
(8) Fukuto, T. R. Mechanism of Action of Organophosphorus and Carbamate Insecticides. *Environ. Health Perspect.* **1990**, *87*, 245−254.
(9) Miao, Y.; He, N.; Zhu, J.-J. History and New Developments of Assays for Cholinesterase Activity and Inhibition. *Chem. Rev.* **2010**, *110*, 5216−5234.
(10) Ellman, G. L. Tissue Sulfhydryl Groups. *Arch. Biochem. Biophys.* **1959**, *82*, 70−77.
(11) Birman, S. Determination of Acetylcholinesterase Activity by a New Chemiluminescence Assay with the Natural Substrate. *Biochem. J.* **1985**, *225*, 825−828.
(12) Rhee, I. K.; van Rijn, R. M.; Verpoorte, R. Qualitative Determination of False-Positive Effects in the Acetylcholinesterase Assay Using Thin Layer Chromatography. *Phytochem. Anal.* **2003**, *14*, 127−131.
(13) Maeda, H.; Matsuno, H.; Ushida, M.; Katayama, K.; Saeki, K.; Itoh, N. 2,4-Dinitrobenzenesulfonyl Fluoresceins as Fluorescent Alternatives to Ellman's Reagent in Thiol-Quantification Enzyme Assays. *Angew. Chem., Int. Ed.* **2005**, *44*, 2922−2925.
(14) Pavlov, V.; Xiao, Y.; Willner, I. Inhibition of the Acetycholine Esterase-Stimulated Growth of Au Nanoparticles: Nanotechnology-Based Sensing of Nerve Gases. *Nano Lett.* **2005**, *5*, 649−653.
(15) Liu, D.; Chen, W.; Tian, Y.; He, S.; Zheng, W.; Sun, J.; Wang, Z.; Jiang, X. A Highly Sensitive Gold-Nanoparticle-Based Assay for Acetylcholinesterase in Cerebrospinal Fluid of Transgenic Mice with Alzheimer's Disease. *Adv. Healthcare Mater.* **2012**, *1*, 90−95.
(16) Peng, L.; Zhang, G.; Zhang, D.; Xiang, J.; Zhao, R.; Wang, Y.; Zhu, D. A Fluorescence "Turn-On" Ensemble for Acetylcholinesterase Activity Assay and Inhibitor Screening. *Org. Lett.* **2009**, *11*, 4014−4017.
(17) Feng, F.; Tang, Y.; Wang, S.; Li, Y.; Zhu, D. Continuous Fluorometric Assays for Acetylcholinesterase Activity and Inhibition with Conjugated Polyelectrolytes. *Angew. Chem., Int. Ed.* **2007**, *46*, 7882−7886.
(18) Li, Y.; Bai, H.; Li, C.; Shi, G. Colorimetric Assays for Acetylcholinesterase Activity and Inhibitor Screening Based on the Disassembly−Assembly of a Water-Soluble Polythiophene Derivative. *ACS Appl. Mater. Interfaces* **2011**, *3*, 1306−1310.
(19) Pardo-Yissar, V.; Katz, E.; Wasserman, J.; Willner, I. Acetylcholine Esterase-Labeled CdS Nanoparticles on Electrodes: Photoelectrochemical Sensing of the Enzyme Inhibitors. *J. Am. Chem. Soc.* **2003**, *125*, 622−623.
(20) Lu, D.; Wang, J.; Wang, L.; Du, D.; Timchalk, C.; Barry, R.; Lin, Y. A Novel Nanoparticle-Based Disposable Electrochemical Immunosensor for Diagnosis of Exposure to Toxic Organophosphorus Agents. *Adv. Funct. Mater.* **2011**, *21*, 4371−4378.
(21) Lévy, R.; Thanh, N. T. K.; Doty, R. C.; Hussain, I.; Nichols, R. J.; Schiffrin, D. J.; Brust, M.; Fernig, D. G. Rational and Combinatorial Design of Peptide Capping Ligands for Gold Nanoparticles. *J. Am. Chem. Soc.* **2004**, *126*, 10076−10084.
(22) Guo, L.; Xu, Y.; Ferhan, A. R.; Chen, G.; Kim, D.-H. Oriented Gold Nanoparticle Aggregation for Colorimetric Sensors with Surprisingly High Analytical Figures of Merit. *J. Am. Chem. Soc.* **2013**, *135*, 12338−12345.
(23) Storhoff, J. J.; Lazarides, A. A.; Mucic, R. C.; Mirkin, C. A.; Letsinger, R. L.; Schatz, G. C. What Controls the Optical Properties of DNA-Linked Gold Nanoparticle Assemblies? *J. Am. Chem. Soc.* **2000**, *122*, 4640−4650.
(24) Li, X.; Peng, L.; Cui, J.; Li, W.; Lin, C.; Xu, D.; Tian, T.; Zhang, G.; Zhang, D.; Li, G. Reactive Photonic Film for Label-Free and Selective Sensing of Cyanide. *Small* **2012**, *8*, 612−618.
(25) Yablonovitch, E. Inhibited Spontaneous Emission in Solid-State Physics and Electronics. *Phys. Rev. Lett.* **1987**, *58*, 2059−2062.
(26) John, S. Strong Localization of Photons in Certain Disordered Dielectric Superlattices. *Phys. Rev. Lett.* **1987**, *58*, 2486−2489.
(27) Aguirre, C. I.; Reguera, E.; Stein, A. Tunable Colors in Opals and Inverse Opal Photonic Crystals. *Adv. Funct. Mater.* **2010**, *20*, 2565−2578.
(28) Zhao, Y.; Xie, Z.; Gu, H.; Zhu, C.; Gu, Z. Bio-Inspired Variable Structural Color Materials. *Chem. Soc. Rev.* **2012**, *41*, 3297−3317.
(29) Ge, J.; Yin, Y. Responsive Photonic Crystals. *Angew. Chem., Int. Ed.* **2011**, *50*, 1492−1522.
(30) Scheid, D.; Lederle, C.; Vowinkel, S.; Schäfer, C. G.; Stühn, B.; Gallei, M. Redox- and Mechano-Chromic Response of Metallopolymer-Based Elastomeric Colloidal Crystal Films. *J. Mater. Chem. C* **2014**, *2*, 2583−2590.
(31) González-Urbina, L.; Baert, K.; Kolaric, B.; Pérez-Moreno, J.; Clays, K. Linear and Nonlinear Optical Properties of Colloidal Photonic Crystals. *Chem. Rev.* **2012**, *112*, 2268−2285.
(32) Schäfer, C. G.; Gallei, M.; Zahn, J. T.; Engelhardt, J.; Hellmann, G. P.; Rehahn, M. Reversible Light-, Thermo-, and Mechano-Responsive Elastomeric Polymer Opal Films. *Chem. Mater.* **2013**, *25*, 2309−2318.
(33) Li, H.; Wang, J.; Yang, L.; Song, Y. Superoleophilic and Superhydrophobic Inverse Opals for Oil Sensors. *Adv. Funct. Mater.* **2008**, *18*, 3258−3264.
(34) Tian, E.; Wang, J.; Zheng, Y.; Song, Y.; Jiang, L.; Zhu, D. Colorful Humidity Sensitive Photonic Crystal Hydrogel. *J. Mater. Chem.* **2008**, *18*, 1116−1122.
(35) Liu, C.; Gao, G.; Zhang, Y.; Wang, L.; Wang, J.; Song, Y. The Naked-Eye Detection of NH_3−HCl by Polyaniline-Infiltrated TiO_2 Inverse Opal Photonic Crystals. *Macromol. Rapid Commun.* **2012**, *33*, 380−385.
(36) Walker, J. P.; Asher, S. A. Acetylcholinesterase-Based Organophosphate Nerve Agent Sensing Photonic Crystal. *Anal. Chem.* **2005**, *77*, 1596−1600.
(37) Tan, E. V.; Lowe, C. R. Holographic Enzyme Inhibition Assays for Drug Discovery. *Anal. Chem.* **2009**, *81*, 7579−7589.
(38) Marrian, D. H. 322. The Reactions of Substituted Maleimides with Thiols. *J. Chem. Soc. (Resumed)* **1949**, 1515−1516.
(39) Ghosh, S. S.; Kao, P. M.; McCue, A. W.; Chappelle, H. L. Use of Maleimide-Thiol Coupling Chemistry for Efficient Syntheses of Oligonucleotide-Enzyme Conjugate Hybridization Probes. *Bioconjugate Chem.* **1990**, *1*, 71−76.
(40) Pounder, R. J.; Stanford, M. J.; Brooks, P.; Richards, S. P.; Dove, A. P. Metal Free Thiol−Maleimide "Click" Reaction as a Mild Functionalisation Strategy for Degradable Polymers. *Chem. Commun.* **2008**, 5158−5160.
(41) Flory, P. J. Statistical Mechanics of Swelling of Network Structures. *J. Chem. Phys.* **1950**, *18*, 108.
(42) Yang, H.; Li, X.; Lan, Y.; Tian, T.; Cui, J.; Zhu, T.; Shen, D.; Li, G. Maleimide-Containing Polymer Inverse Opals: A New Kind of Reactive Photonic Structure with Significant Extendibility. *J. Mater. Chem. C* **2013**, *1*, 6120−6128.
(43) Zhao, Y.; Zhao, X.; Gu, Z. Photonic Crystals in Bioassays. *Adv. Funct. Mater.* **2010**, *20*, 2970−2988.
(44) Takeoka, Y.; Watanabe, M. Polymer Gels That Memorize Structures of Mesoscopically Sized Templates. Dynamic and Optical Nature of Periodic Ordered Mesoporous Chemical Gels. *Langmuir* **2002**, *18*, 5977−5980.
(45) Mantovani, G.; Lecolley, F.; Tao, L.; Haddleton, D. M.; Clerx, J.; Cornelissen, J. J. L. M.; Velonia, K. Design and Synthesis of N-Maleimido-Functionalized Hydrophilic Polymers via Copper-Medi-

ated Living Radical Polymerization: A Suitable Alternative to PEGylation Chemistry. *J. Am. Chem. Soc.* **2005**, *127*, 2966−2973.
(46) Aguiar, E. C.; da Silva, J. B. P.; Ramos, M. N. A Theoretical Study of the Vibrational Spectrum of Maleimide. *J. Mol. Struct.* **2011**, *993*, 431−434.
(47) Haddad, G. L.; Young, S. C.; Heindel, N. D.; Bornhop, D. J.; Flowers, R. A. Back-Scattering Interferometry: An Ultrasensitive Method for the Unperturbed Detection of Acetylcholinesterase−Inhibitor Interactions. *Angew. Chem., Int. Ed.* **2012**, *51*, 11126−11130.
(48) Larsson, R.; Pei, Z.; Ramström, O. Catalytic Self-Screening of Cholinesterase Substrates from a Dynamic Combinatorial Thioester Library. *Angew. Chem., Int. Ed.* **2004**, *43*, 3716−3718.
(49) Lineweaver, H.; Burk, D. The Determination of Enzyme Dissociation Constants. *J. Am. Chem. Soc.* **1934**, *56*, 658−666.
(50) Wang, M.; Gu, X.; Zhang, G.; Zhang, D.; Zhu, D. Convenient and Continuous Fluorometric Assay Method for Acetylcholinesterase and Inhibitor Screening Based on the Aggregation-Induced Emission. *Anal. Chem.* **2009**, *81*, 4444−4449.
(51) Nakayama, D.; Takeoka, Y.; Watanabe, M.; Kataoka, K. Simple and Precise Preparation of a Porous Gel for a Colorimetric Glucose Sensor by a Templating Technique. *Angew. Chem., Int. Ed.* **2003**, *42*, 4197−4200.
(52) Wang, X.; Mu, Z.; Liu, R.; Pu, Y.; Yin, L. Molecular Imprinted Photonic Crystal Hydrogels for the Rapid and Label-Free Detection of Imidacloprid. *Food Chem.* **2013**, *141*, 3947−3953.
(53) Meng, L.; Meng, P.; Zhang, Q.; Wang, Y. Fast Screening of Ketamine in Biological Samples Based on Molecularly Imprinted Photonic Hydrogels. *Anal. Chim. Acta* **2013**, *771*, 86−94.